Geoscientific
Model Development

Open Access

EGU

Supplement of

Development of the WRF-CO2 4D-Var assimilation system v1.0

Tao Zheng et al.

Correspondence to: Tao Zheng (zheng1t@cmich.edu)
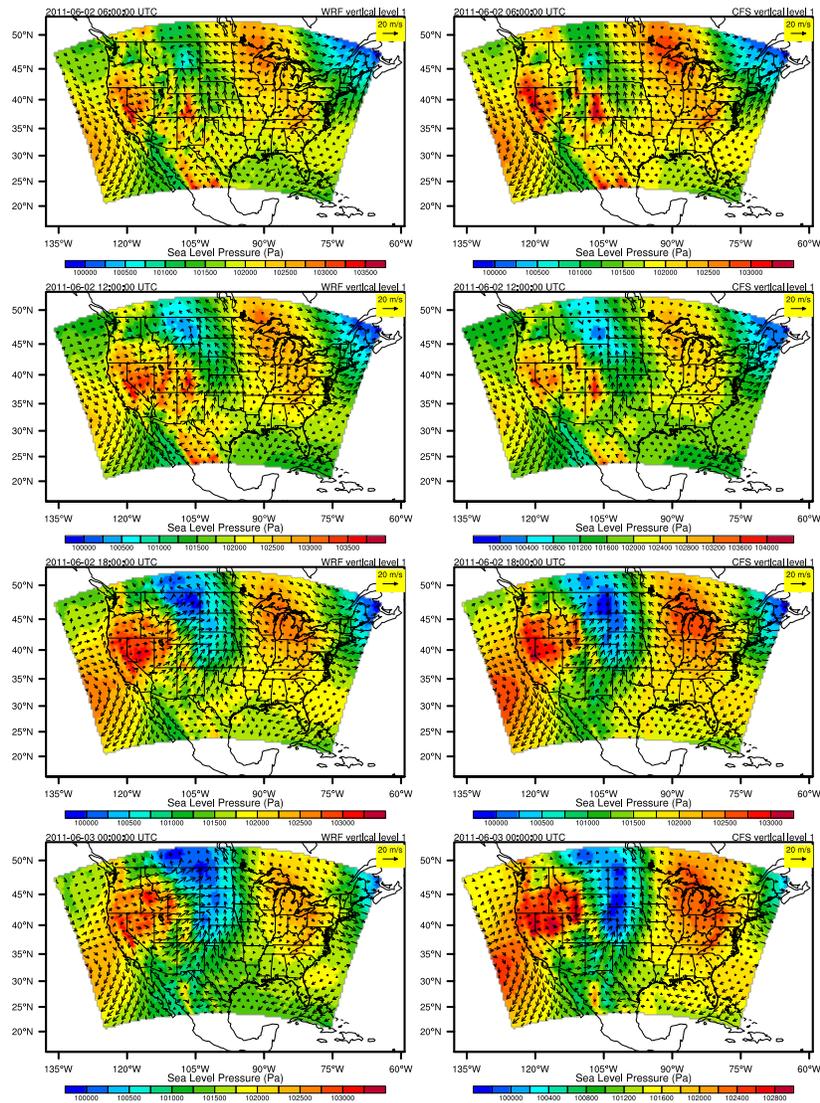
Figure 1: Sea level pressure (background) and horizontal wind (arrows) at the first vertical level simulated by WRF (left column) and interpolated from CFSv2 (right column). Figures are plotted at 6-hour interval for the 24-hour simulation period staring at 2011-06-02 00:00 UTC.
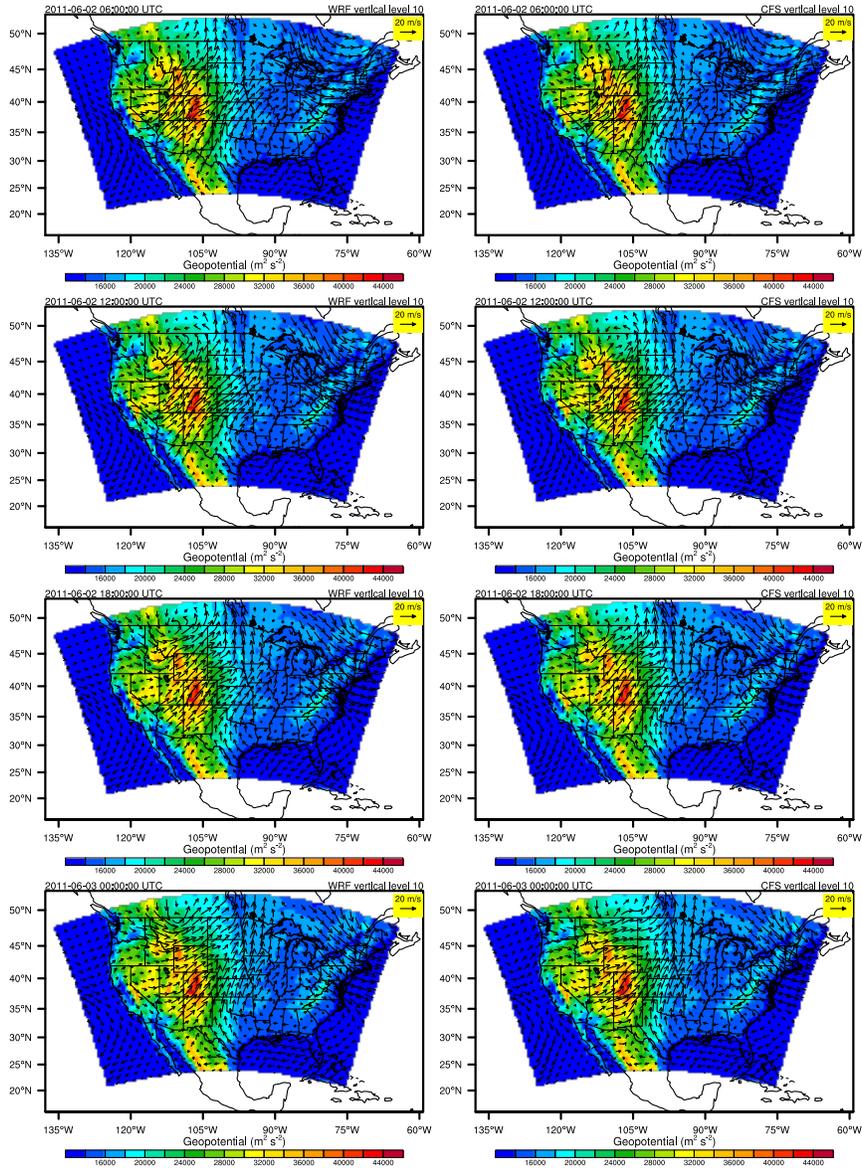
Figure 2: Geopotential (background) and horizontal wind (arrows) at the 10$^{\text{th}}$ vertical level simulated by WRF (left column) and interpolated from CFSv2 (right column). Figures are plotted at 6-hour interval for the 24-hour simulation period staring at 2011-06-02 00:00 UTC.
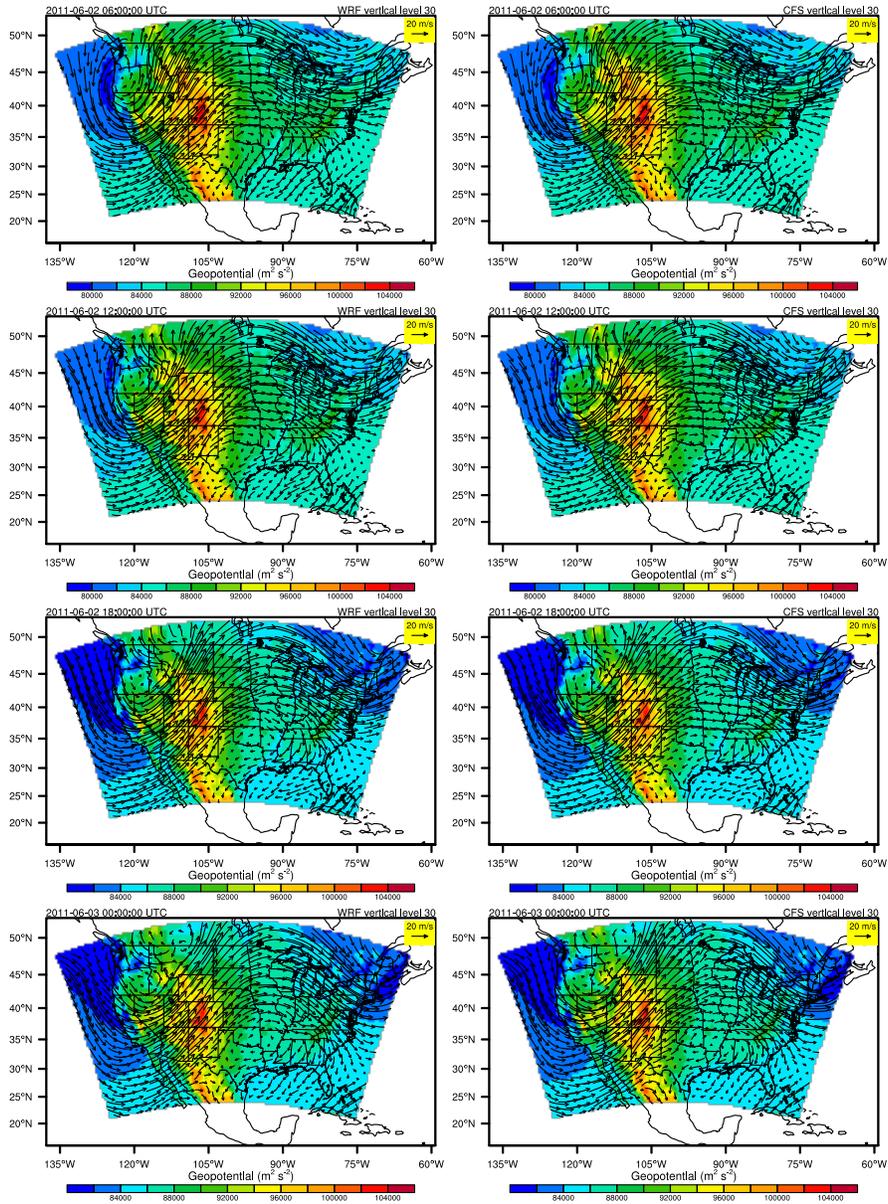
Figure 3: Geopotential (background) and horizontal wind (arrows) at the 30th vertical level simulated by WRF (left column) and interpolated from CFSv2 (right column). Figures are plotted at 6-hour interval for the 24-hour simulation period staring at 2011-06-02 00:00 UTC.
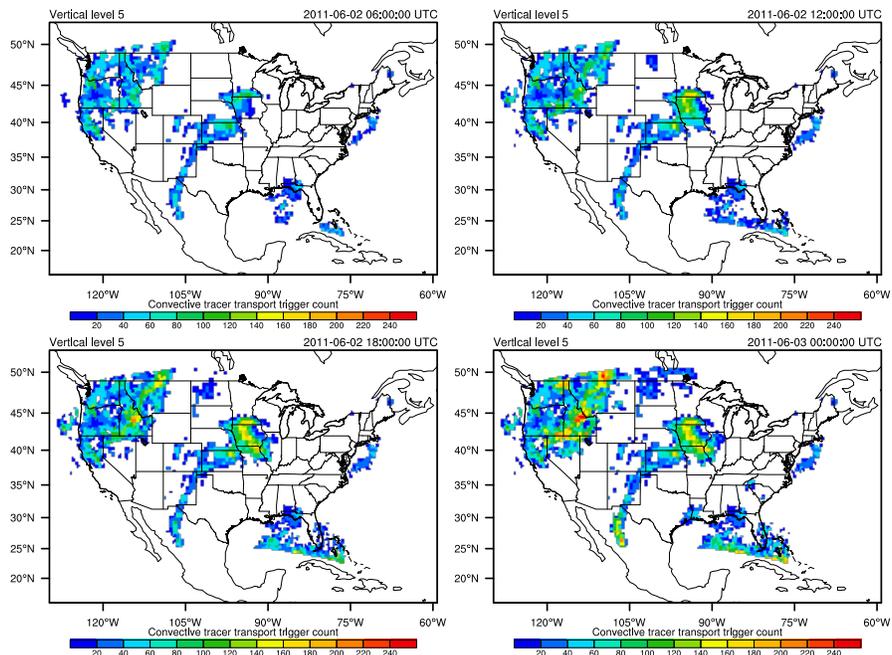
Figure 4: Convective tracer transport trigger count at the 5th vertical level plotted at 6-hour interval.
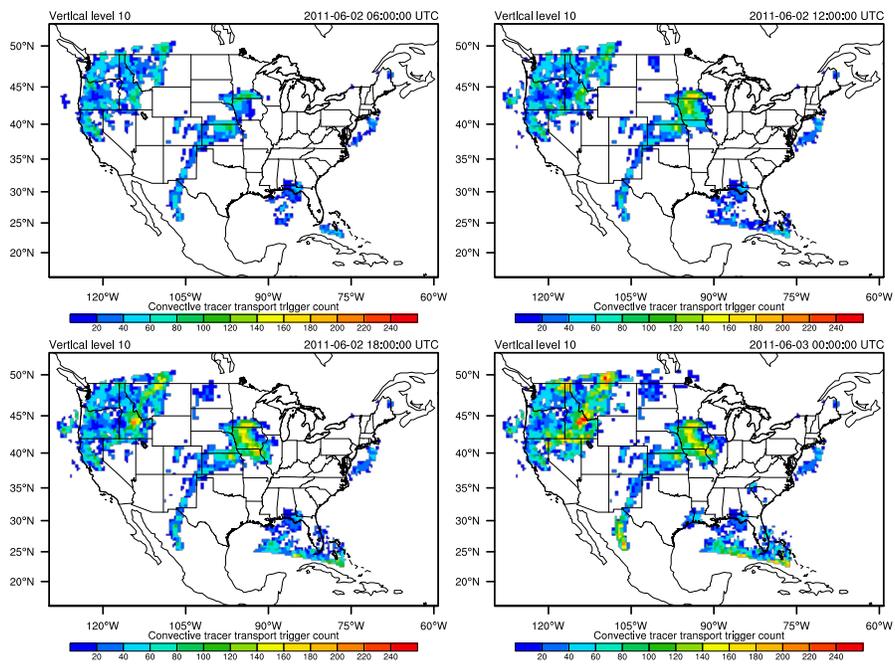
Figure 5: Same as Fig. 4, but for the 10th level.
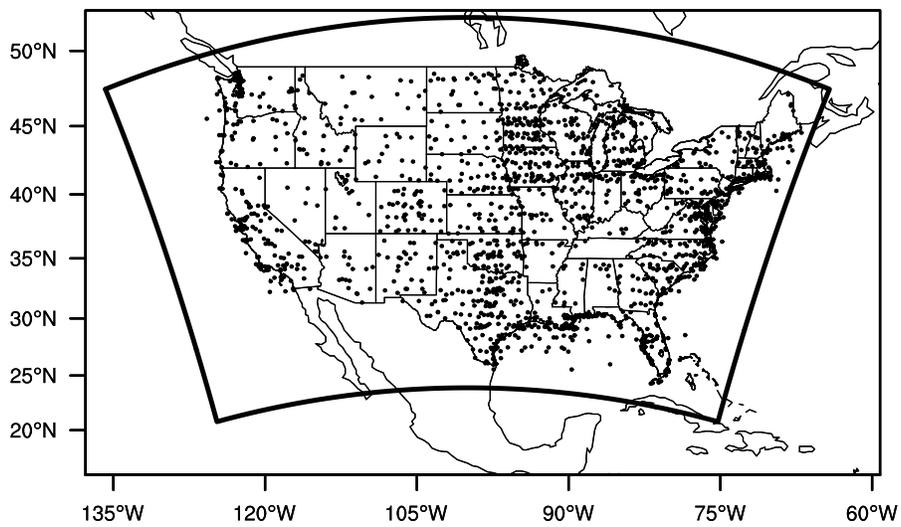
Figure 6: Locations of the meteorological stations used for evaluating the WRF simulation. The bold dark outline marks the boundary of the WRF simulation domain. The surface meteorological data are obtained from NOAA Integrated Surface Dataset.
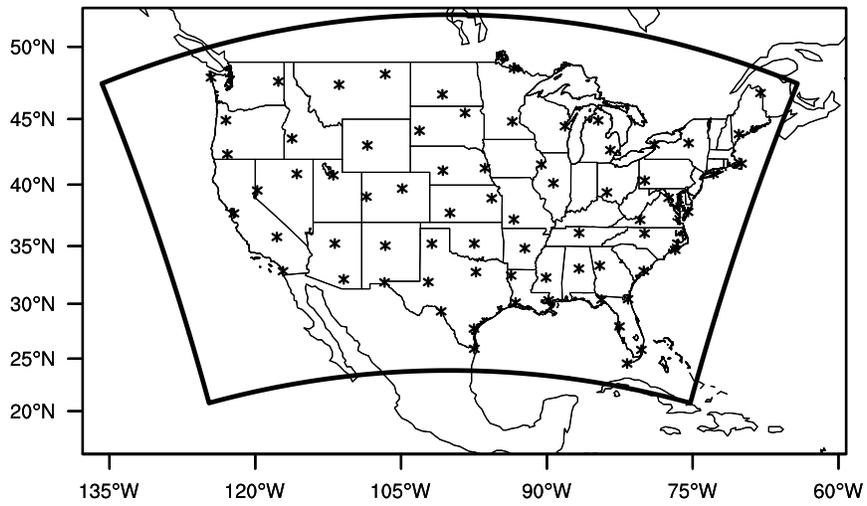
Figure 7: Locations of the radiosonde stations used for evaluating the WRF simulation. The bold dark outline marks the boundary of the WRF simulation domain. The radiosonde data are obtained from NOAA/ESRL radiosonde database